

PASSIVE PLASMA LENS EXPERIMENTS AT FACET-II

S. Meng*, C. Hansel, V. Lee, M. Litos, E. Ros, University of Colorado Boulder, Boulder, CO, USA
 E. Adli, G. J. Cao, University of Oslo, Oslo, Norway
 R. Ariniello, C. Emma, S. Gessner, M. J. Hogan, A. Knetsch, N. Majernik, B. O'Shea, D. Storey
 SLAC National Accelerator Laboratory, Menlo Park, CA, USA
 S. Corde, LOA, ENSTA Paris, CNRS, Ecole Polytechnique,
 Institut Polytechnique de Paris, Palaiseau, France
 C. E. Doss, Lawrence Berkeley National Laboratory, Berkeley, CA, USA
 T. N. Dalichaouch, C. Joshi, K. A. Marsh, C. Zhang
 University of California Los Angeles, Los Angeles, CA, USA

Abstract

The beam-driven, passive plasma lens can provide axisymmetric focusing with strengths orders of magnitude greater than conventional quadrupole magnets, while remaining ultra-compact. These characteristics make it attractive for beam matching into a plasma wakefield accelerator and for controlling beam divergence downstream of plasma stages. Optimal performance can be achieved in the underdense regime, resulting in a linear focusing force and emittance preservation of the focused beam. We report progress on experimental results from SLAC's FACET-II facility, where we utilized a fs Ti:Sapphire laser pulse to ionize hydrogen gas from a supersonic gas jet to focus several hundred pCs of charge of a 10 GeV electron beam.

INTRODUCTION

A plasma wakefield accelerator (PWFA) can produce accelerating gradients orders of magnitude stronger than those of conventional radio-frequency structures, which allows development of compact accelerators that can benefit future colliders and light sources. Several milestones have been achieved to demonstrate high energy gain, high efficiency acceleration, and low energy spread beam [1–3]. Moving toward future accelerators, preserving emittance in a PWFA stage is crucial for achieving high luminosity in colliders and high brightness in light sources.

In a PWFA, a leading electron drive bunch generates a strong longitudinal wakefield that can accelerate a trailing witness bunch. To prevent emittance growth caused by chromatic phase mixing of the witness bunch, its Twiss parameter β must be matched according to the condition $\beta = \sqrt{2\gamma_b/k_p}$, where γ_b is the Lorentz factor of the electron bunch and k_p is the plasma wave number. For a 10 GeV electron bunch and a $1 \times 10^{16} \text{ cm}^{-3}$ plasma density, a typical parameter at the FACET-II facility at SLAC National Accelerator Laboratory, the required β at the entrance of the PWFA stage is about 1 cm. Achieving such a small value is challenging with conventional electromagnetic quadrupole magnets. Several approaches have been proposed to provide such strong focusing, with one prevalent method being the use of a plasma

density ramp [4, 5]. However, this approach typically requires a long plasma matching section and precise control of the plasma density profile. Hence, the use of plasma lens has been discussed [6], providing focusing gradients on the order of MT/m, which can significantly shorten the plasma ramp section and thus allows efficient phase-space matching.

The proposed plasma lens experiment at FACET-II aims to realize a specific type of plasma lens [6, 7]. Its strong focusing arises from the transverse wakefield generated by the drive bunch. The lens is thin so that the witness bunch experiences minimal energy gain. Ideally, the lens operates in the underdense regime, where the drive bunch density $n_b > n_p$, allowing it to generate an electron-depleted ion column in which the emittance of the witness bunch can be preserved. In this paper, we report preliminary results of a submillimeter, beam-driven, passive plasma lens using a pre-formed, laser-ionized plasma. The peak focusing gradient is approximately 0.4 MT/m, which is orders of magnitude stronger than conventional quadrupoles (1 T/m), permanent magnet quadrupoles (500 T/m [8]), and active plasma lenses (3.5 kT/m [9, 10]).

EXPERIMENTAL SETUP

The experimental setup, shown in Fig. 1, uses a two-bunch electron beam generated by a notch collimator, with the drive bunch carrying a charge of 780 pC and the witness bunch 650 pC. The plasma lens is pre-formed by ionizing neutral hydrogen gas from a supersonic jet using a 3 mJ, [insert pulse duration] fs Ti:sapphire laser. The laser propagates transversely to the beamline, so the electron beam traverses the plasma width, resulting in a thin lens configuration. A simulated initial plasma density profile using the experimental laser parameter is shown in Fig. 2 where the initial plasma width is only 132 μm . The delay between the laser pulse and the arrival of the electron beam can be adjusted to allow plasma expansion, thereby increasing the plasma length for stronger lensing and reducing the plasma density to reach the underdense regime easier.

The gas jet (see Fig. 1 (b)) is a canonical de Laval nozzle, operating at 50 psi and placed 1.5 cm below the electron beam. Detailed specifications of the nozzle are provided in the paper [11]. The neutral hydrogen gas profile is calibrated through simulations using ANSYS Fluent, with the resulting

* shutang.meng@colorado.edu

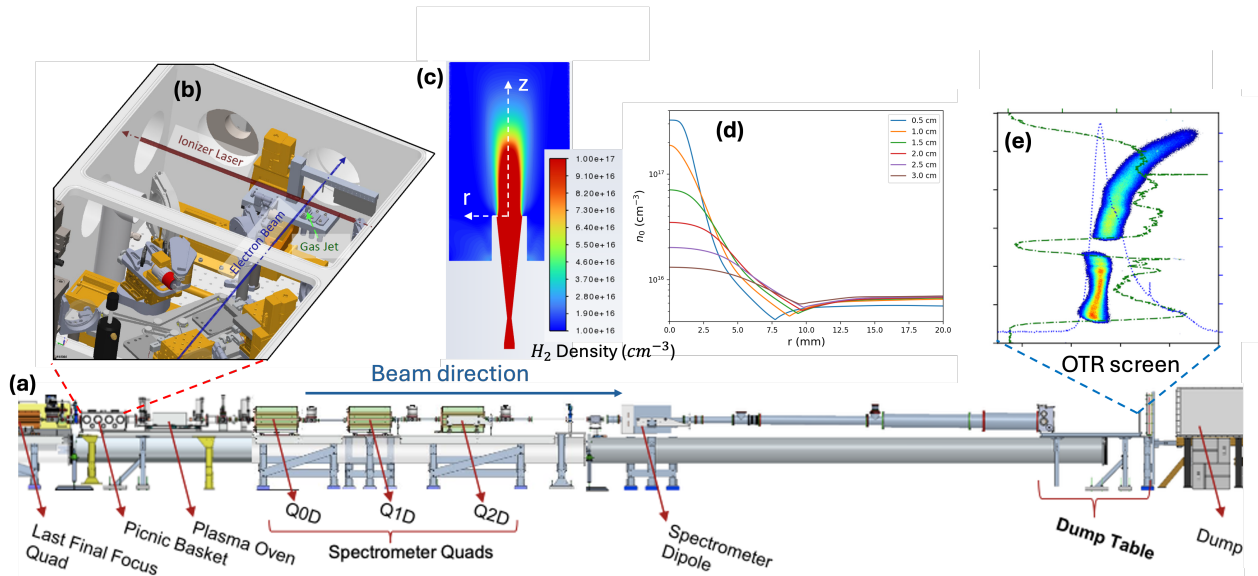


Figure 1: Experimental setup. (a) A two-bunch electron beam travels from left to right and is first focused by four final-focus quadrupoles. (b) The plasma lens is formed by laser ionization of neutral hydrogen from a supersonic gas jet, using a femtosecond Ti:Sa laser that propagates transversely to the electron beam. (c) The gas jet density profile is calibrated via fluid simulations using ANSYS Fluent, with radial density profile lineouts at various heights shown in (d). After interacting with the plasma lens, the electron bunch is transported to the dump table through three spectrometer quadrupoles and a dipole magnet. The transverse profile in the horizontal dimension x is imaged on an optical transition radiation (OTR) screen, as shown in (e).

density contour shown in Fig. 1 (c) and radial density profile lineouts at various heights above the nozzle shown in Fig. 1 (d). Since the plasma lens operates over a submillimeter scale, the neutral density profile of the lens before ionization can be considered approximately uniform.

the OTR screen to measure beam spot size evolution after exiting the plasma lens. Additionally, multishot emittance measurements are conducted using quadrupole scans, imaging plasma lens exit.

Plasma Characterization

To observe a clear plasma lensing effect, with a focal length located approximately 10–20 cm downstream and a significant reduction in beam spot size, particle-in-cell (PIC) simulations indicate that a plasma length of about 500 μm is required at a density of $1 \times 10^{16} \text{ cm}^{-3}$. However, the initial plasma profile shown in Fig. 2 is only on the order of 100 μm . To overcome this, the plasma is initially ionized at a higher density and allowed to expand, thereby producing a longer profile at a lower density. In this experiment, the delay between the laser pulse and the electron beam arrival is set to 3 ns.

The plasma length can be measured by scanning the laser height above the gas jet and monitoring the beam–plasma interaction. In a plasma lens, the divergence of the witness bunch serves as a proxy for interaction strength. Beam divergence is measured using parallel-to-point imaging on the OTR screen, as shown in Fig. 3. The images clearly show that the witness bunch exhibits significantly higher divergence increase when the plasma lens is active. By varying the laser height, we observe a transition from no plasma interaction (similar to the lens-off image), to maximum interaction, and back to no interaction. This transition region provides a rough estimate of the plasma length, which is

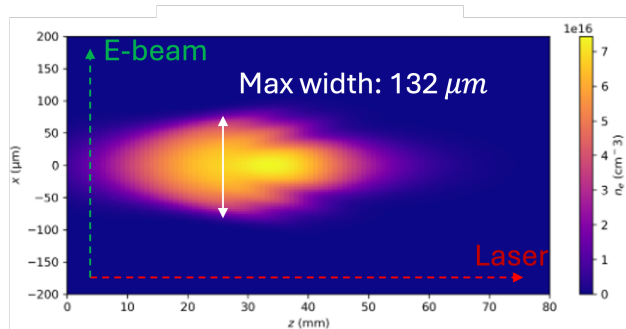


Figure 2: The formation of the initial plasma profile via laser ionization of the hydrogen gas is simulated. For a 3 mJ laser pulse, the plasma width reaches a maximum of approximately 132 μm .

After interacting with the plasma lens, the drive and witness bunches are transported through three spectrometer quadrupole magnets and a dipole magnet that provides vertical (y -direction) energy dispersion. As a result, the optical transition radiation (OTR) screen (see Fig. 1 (e)) can capture the energy spectrum as a function of the transverse x -profile with high resolution. In the experiment, object plane scans are performed with the imaging plane fixed at

found to be $400 \pm 100 \mu\text{m}$. The primary source of uncertainty is the finite laser spot size.

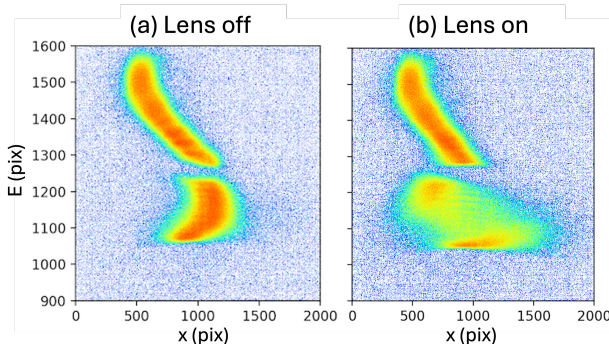


Figure 3: Parallel-to-point images on the OTR screen with the plasma lens turned on (b) and off (a). The object and imaging planes are fixed at the plasma lens exit and the OTR screen, respectively, with the spectrometer set to image the 10 GeV energy.

RESULTS & DISCUSSION

In the data analysis, the witness bunch is divided into five energy slices, each spanning approximately 40 MeV energy range and containing more than 100 pC of charge. Preliminary results of the beam spot size evolution downstream of the lens are presented in Fig. 4 (a). It is important to note that chromaticity in the spectrometer has not been corrected in the data analysis. This limitation notably affects the apparent beam waist location for off-energy slices. Nevertheless, strong plasma lensing can be observed. As shown in Fig. 4 (b), a comparison between the lens-on and lens-off cases for one of the five energy slices reveals a significant reduction in beam size. Similar behavior is observed across all slices, with the minimum spot size ranging from 20 μm down to 14 μm .

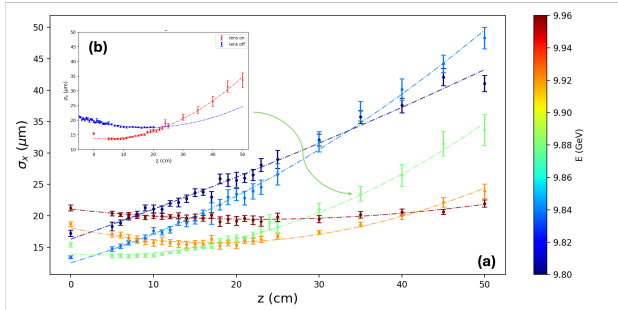


Figure 4: Evolution of the RMS beam size σ_x downstream of the plasma lens. The position $z = 0$ corresponds to the lens exit. In (a), the σ_x evolution with the plasma lens on is shown for five binned energy slices of the witness bunch, with the center energy of each slice indicated by the colorbar. Panel (b) compares the lens-on and lens-off cases for the energy slice centered at 9.88 GeV.

A preliminary emittance analysis based on quadrupole scan data indicates that the normalized RMS emittance $\epsilon_{x,n,\text{rms}}$ of the witness bunch ranges from 8 to 12 $\mu\text{m rad}$ from head to tail before entering the plasma lens. Inside the lens, the bunch experiences an emittance growth of approximately 40% to 90%, increasing from head to tail. Further analysis is required to quantify the emittance growth more precisely and to assess its implications for beam quality and phase-space preservation. Based on simulations, we believe the observed emittance growth is largely owed to nonlinear focusing forces caused by plasma interaction in quasilinear regime. Using the values obtained from the emittance measurement, the peak reduction of the beta function β_x in one energy slice is observed to decrease from approximately 75 cm to 21 cm, corresponding to a 72% reduction. The focusing strength is numerically calculated to be $13,100 \text{ m}^{-2}$, which corresponds to an equivalent quadrupole gradient of 0.437 MT/m.

CONCLUSION

In this paper, we demonstrate a beam-driven, thin passive plasma lens capable of achieving a focusing gradient of 0.4 MT/m for more than 100 pC of charge in a 10 GeV electron beam. A maximum β reduction exceeding 72% is observed. These results highlight the potential of passive plasma lens for achieving the matching conditions required in a PWFA. They also represent a significant step forward in the realization of a thin, underdense, passive plasma lens capable of preserving the emittance of the witness bunch. Further analysis is needed to reconstruct the beam spot size evolution with chromatic correction and to quantify the emittance evolution. Additional PIC simulations are required to model the realistic beam–plasma interaction and the plasma expansion from the initial laser-ionized profile.

ACKNOWLEDGEMENTS

We thank SLAC National Accelerator Laboratory for providing beam time at the FACET-II User Facility. We also thank S. Walcott for simulation support. This material is based on work supported by the National Science Foundation Award Number PHY-1806053 and Faculty Early Career Development Program Award Number PHY-2047083 and the U.S. Department of Energy, Office of Science, Office of High Energy Physics, Award Number DE-SC001796.

REFERENCES

- [1] I. Blumenfeld *et al.*, “Energy doubling of 42 GeV electrons in a metre-scale plasma wakefield accelerator”, *Nature*, vol. 445, no. 7129, pp. 741–744, 2007. doi:10.1038/nature05538
- [2] M. Litos *et al.*, “High-efficiency acceleration of an electron beam in a plasma wakefield accelerator”, *Nature*, vol. 515, no. 7525, pp. 92–95, 2014. doi:10.1038/nature13882

- [3] C. A. Lindström *et al.*, “Energy-spread preservation and high efficiency in a plasma-wakefield accelerator”, *Phys. Rev. Lett.*, vol. 126, no. 1, 2021.
doi:10.1103/physrevlett.126.014801
- [4] X. L. Xu *et al.*, “Physics of phase space matching for staging plasma and traditional accelerator components using longitudinally tailored plasma profiles”, *Phys. Rev. Lett.*, vol. 116, no. 12, 2016. doi:10.1103/physrevlett.116.124801
- [5] R. Ariniello, C. E. Doss, K. Hunt-Stone, J. R. Cary, and M. D. Litos, “Transverse beam dynamics in a plasma density ramp”, *Phys. Rev. Accel. Beams*, vol. 22, no. 4, 2019.
doi:10.1103/physrevaccelbeams.22.041304
- [6] C. E. Doss *et al.*, “Laser-ionized, beam-driven, underdense, passive thin plasma lens”, *Phys. Rev. Accel. Beams*, vol. 22, no. 11, 2019.
doi:10.1103/physrevaccelbeams.22.111001
- [7] C. E. Doss *et al.*, “Underdense plasma lens with a transverse density gradient”, *Phys. Rev. Accel. Beams*, vol. 26, no. 3, 2023. doi:10.1103/physrevaccelbeams.26.031302
- [8] J. K. Lim *et al.*, “Adjustable, short focal length permanent-magnet quadrupole based electron beam final focus system”, *Phys. Rev. Spec. Top. - Accel. Beams*, vol. 8, no. 7, 2005.
doi:10.1103/physrevstab.8.072401
- [9] J. van Tilborg *et al.*, “Active plasma lensing for relativistic laser-plasma-accelerated electron beams”, *Phys. Rev. Lett.*, vol. 115, no. 18, 2015.
doi:10.1103/physrevlett.115.184802
- [10] K. N. Sjobak *et al.*, “Strong focusing gradient in a linear active plasma lens”, *Phys. Rev. Accel. Beams*, vol. 24, no. 12, 2021. doi:10.1103/physrevaccelbeams.24.121306
- [11] C. Zhang *et al.*, “Ionization induced plasma grating and its applications in strong-field ionization measurements”, *Plasma Phys. Control. Fusion*, vol. 63, no. 9, p. 095 011, 2021.
doi:10.1088/1361-6587/ac1751